Efficient elimination of tyrosol in a zero valent iron-EDTA system at mild conditions

Dongmei Fu [a,#], Selamawit A. Messele [a], Agustí Fortuny [b], Frank Stüber [a], Azael Fabregat [a], Josep Font [a] and Christophe Bengoa [a,*]

[a] Departament d'Enginyeria Química, Escola Tècnica Superior d'Enginyeria Química, Universitat Rovira i Virgili, Av. Països Catalans 26, 43007 Tarragona, Catalonia, SPAIN

[b] Departament d'Enginyeria Química, EPSEVG, Universitat Politècnica de Catalunya, Av. Víctor Balaguer s/n, 08800 Vilanova i la Geltrú, Barcelona, Catalonia, SPAIN

* Corresponding author. Tel.: +34-977-558619; fax: +34-977-559667.
E-mail address: christophe.bengoa@urv.cat

[#] Present address: Dalian Institute of Chemical Physics, Chinese Academy of Sciences, Dalian 116023, China

Abstract

This study investigates the degradation of tyrosol, a major compound of the polyphenolic fraction present in olive oil mill wastewater (OMW) by means of a zero valent iron/air Fenton like system in presence of EDTA. To the best of our knowledge it is the first time that this process is entirely devoted to tyrosol and in the effect of its experimental conditions. Reaction conditions, i.e., load of iron, concentration of EDTA, temperature and initial pH, are examined. The concentration of EDTA, the load of Fe and the temperature have a great

influence on tyrosol degradation. The experimental results show that tyrosol can be removed efficiently. Above 99% of tyrosol conversion was achieved after 2 h with 0.2 mM tyrosol, 0.45 mM EDTA, 90 g/L of zero valent iron at 30 ºC, whereas TOC removal was 80% after 3 h at the above reaction conditions. Unlike classical Fenton, Fe-EDTA oxidation system can be used in a broad pH range, from 3 to 8. Kinetic analysis using a Langmuir-Hinshelwood (LH) model shows good fitting to the experimental data. The activation energy estimated, 37.7 kJ/mol, was close to that of other phenolic compounds. In addition, the EDTA rate constant obtained by model, 0.05 min^{-1} (20ºC), was in accordance with other studies. A simplified mechanism for the degradation of tyrosol is presented, where some reaction intermediates were identified.

Keywords

Tyrosol oxidation, olive mill wastewater, zero valent iron, EDTA, Fenton like process, Langmuir-Hinshelwood (LH) model

1. Introduction

The expansion of the olive oil industry in the main olive-producing countries of the Mediterranean region such as Spain, Italy, Greece, Portugal, Tunisia and Turkey, produces huge amounts of wastewater known as olive mill wastewater, OMW [1]. Because of its high content of organic substances (14-15%) and phenols (up to 10 g/L), OMW is one of the crucial environmental issues in the Mediterranean basin [2]. OMW has a very high organic load and especially the presence of acidic and phenolic compounds that are major contributors to the unusual toxicity and antibacterial activity of this wastewater [3, 4].

The management of OMW and other similar agro-industrial effluents is a complicated and worth to be resolved issue with serious socio-economic implications. In the last few years,

many OMW treatment systems have been proposed. Among them, physical processes such as adsorption [5], thermal evaporation [6], electro coagulation [7], flocculation [8] and membrane filtration [9] have been considered, but these methods have one major disadvantage since they do not provide a real destruction of the compounds but only transfer them from a diluted to a concentrated stream which needs further treatment.

Biological treatments, such as aerobic and anaerobic digestions, have been also developed for the treatment of OMW [10]. However, due to the inhibitory effect of polyphenols, many problems concerning the high toxicity and inhibition of biodegradation have been encountered during the biological treatment [2, 11]. One possible solution to avoid the problems of biological processes is combining them with others processes like AOPs [12].

Advanced Oxidation Processes (AOPs) are increasingly used in the destruction of environmental pollutants and reduction of COD level of OMW. Among them, Fenton [1] and photo-Fenton peroxidation [13], ozonation [14] or sonication [15] have been successfully tested recently.

Alternatively, Fenton like systems using zero valent iron, ethylenediaminetetraacetate (EDTA) and air (ZEA method) were developed for organic pollutants degradation [16]. EDTA, a widely used chelating agent, was found to help breaking down the O-O bond of molecular oxygen and produce H_2O_2 and radicals $OH\cdot$ in the Fe/EDTA system [17]. Compared to the traditional Fenton oxidation system, this process is both unique and simple in the sense that the oxidative system adds only iron metal, EDTA and air to the aqueous stream containing the target organic pollutant and can activate oxygen at room temperature. On the other hand, it has to be noticed that EDTA itself is also degraded by the system zero valent iron and air [17, 18]. This fact signifies that there is a competition to degrade both organics: contaminant and EDTA. This system has previously shown to be capable of degrading a variety of organic pollutants, including olive mill wastewaters [19]. One of the major concerns regarding OMW

76 treatment is that they are strong wastes, the concentrations of phenolic compounds are very
77 high, up to 10 g/L and, they are difficult to remove by biological degradation because their
78 toxicity [20]. On the other hand, tyrosol is one of the three phenolic compounds in highest
79 concentration in olive oil. The concentration of tyrosol in extra-virgin olive oil is up to 27±4
80 mg/kg of oil [21]. For this reason, tyrosol can be considered as a good model for the treatment
81 of olive mill wastewater. Tyrosol (*p*-Hydroxyphenylethanol) exhibits toxicity towards several
82 microorganisms [22]. In addition the tyrosol oxidation studies are very scarce compared to
83 phenol, p-coumaric acid or p-hydroxybenzoic acid studies. Anyway, it was reported the
84 resistance of tyrosol to oxidation even by an individual electro-Fenton experiment after 4 h
85 [23], or a conversion of only 45%, using a combination of UV radiation and rose Bengal as a
86 photo sensitizer after 15 h of reaction [24]. However, photocatalytic oxidation of tyrosol over
87 UV/H_2O_2/(Al-Fe) PILC was able to attain 100 % conversion with 50% TOC reduction at pH
88 3, λ = 254 nm, 20 mM H_2O_2 but only after 24 h reaction [25]. More recently, catalytic wet
89 peroxide oxidation of tyrosol was able to totally oxidize the pollutant with 80% of TOC
90 removal after 1 h reaction at 25ºC [26].
91 Finally, a study of degradation of six model olive mill contaminants of OMW catalysed by
92 zero-valent iron with nitrilotriacetic acid disodium salt as chelant and air was performed [27].
93 This study evaluated the feasibility of the utilisation of ZVI with a chelant and oxygen for the
94 elimination of the contaminants alone (350 mg/L) and in a mixture (1000 mg/L). Mixtures
95 total organic contaminant, COD and TOC conversions were always up to 92, 84 and 44%
96 respectively, demonstrating the effectiveness of the technique. Compared to the direct use of
97 H_2O_2 as oxidant for the degradation of pollutants, the ZEA system is cheap, as it uses air as
98 oxidant and a low cost catalyst, easily available, not needing previous preparation.
99 The objective of the present work is to study intensively the effectiveness of the treatment at
100 mild conditions of chelated ZVI and air on tyrosol, a toxic and recalcitrant pollutant, a

representative compound contained in OMW. The effect of initial concentration of tyrosol, initial concentration of EDTA, initial mass of zero valent iron (ZVI), temperature and pH was evaluated for tyrosol removal.

2. Materials and methods

2.1. Materials and reagents

Tyrosol was purchased from Fluka (>98% purity, ref. 188255). Granulated metallic zero valent iron (ref. 211934) was purchased from Panreac. Ethylenediaminetetraacetate disodium salt bi-hydrate was also purchased from Panreac (EDTA, 98% purity, ref. 131669). The main physico-chemical properties of tyrosol and EDTA are presented in Table 1. All other analytical grade chemicals and HPLC purity grade solvents were purchased from Sigma-Aldrich. Deionised water (Millipore, Milli-Q) was used to prepare all aqueous solutions. The initial pH values were adjusted by the addition of diluted aqueous solutions of HCl and NaOH.

2.2. Experimental set-up and procedure

A 200 mL jacketed stirred batch reactor was used for all oxidation runs. The Figure 1 presents a schematic diagram of the reactor. The reaction temperature was controlled by circulating water from a thermostatic bath through the jacket. The reactor was filled with 100 mL of either 2 mM, 4mM or 8 mM (0.28 g/L, 0.56 g/L, 1.12 g/L, respectively) tyrosol solution and heated to the desired temperature (from 20 to 50ºC). Then, the compressed air was fed and the air flow was set to 10 NL/h using a rotameter (KROHNE) equipped with a valve. This flow of air is sufficient to keep at saturation the oxygen dissolved in the solution. A porous glass at the end of the air pipe, placed at the bottom of the reactor, allowed the formation of well distributed small air bubbles. A volume of 0.5 to 2.0 mL of 30 mM EDTA solution was added to the reactor to attain the EDTA concentration desired (from 0.15 to 0.60 mM). Finally, the

mechanical stirrer was set to 300 rpm and ZVI was added to start the reaction (ZVI mass from 10 to 90 g/L). Liquid samples, 5 mL, were withdrawn at intervals, filtered through 0.45 μm nylon membrane filters (Teknokroma, ref. TR-200101) and then analyzed by HPLC. The pH was measured with a MPC 227 pH meter. Some experiments were conducted three times to check the reproducibility of results and the agreement (within ±3%) between successive experiments was considered satisfactory.

2.3. Analytical Procedures

2.3.1. High Performance Liquid Chromatography (HPLC)

The liquid samples were analyzed by HPLC using Agilent 1100 series HPLC-DAD system on a Hypersil ODS C18 column (250×4.6 mm). The mobile phase was methanol/water (pH 1.41 adjusted with sulphuric acid) 15/85 (v/v) at a flow rate of 1.0 mL/min while 280 nm wavelength was fixed for detection. The injection volume was 5 μL. Under these conditions, the retention time of tyrosol was 7.8 min. Linearity of the detector response was verified with tyrosol standard solution prepared in ultra pure water over the range from 1 mg/L to 200 mg/L. The calibration showed good linearity, the correlation coefficient (r) being almost identical and > 0.999. The chromatographic peak of tyrosol for a concentration of 1 mg/L was well over the limit of detection of the equipment. This limit was not determined quantitatively.

Some of the reaction intermediates (acetic acid, formic acid, pyruvic acid, succinic acid, 3,4-dihydroxyphenylethanol, 3,4-dihydroxyphenylacetic acid and 3,4-dihydroxymandelic acid) were analyzed using the methodology described elsewhere [28].

2.3.2. Total Organic Carbon (TOC)

Total organic carbon (TOC) analysis was performed in an automatic TOC Analyser (Analytic

Jena, model NC 2100). Prior to the analysis, the samples were acidified with 50 mL HCl 2 N, bubbled with synthetic air for 3 min to remove the inorganic carbon content and then injected to the analyser.

2.3.3. Atomic Absorption Spectroscopy

The dissolved iron content of the samples was determined using Atomic Absorption Spectroscopy (AAS) in an ANALYST 300 Perkin-Elmer Spectrophotometer. The liquid samples were also filtered with a syringe filter of 0.45 μm nylon (Teknokroma, ref.TR-200101). Then the amount of Fe cations in the reaction media was detected and quantified by using AAS at 249nm. Prior to analysis, a calibration curve was prepared using the absorbance of standard solutions.

2.4. Characterization of the zero valent iron

BET surface areas were calculated measuring N_2-physisorption adsorption-desorption isotherms at 77 K, using Micromeritics ASAP 2000 surface analyzer. Before analysis, the sample was degassed in vacuum at 393 K for 6 hours.

3. Results and Discussion

3.1. Preliminary tests

An initial set of tyrosol oxidation experiments was conducted as proof of concept. The initial tyrosol concentration was 2 mM and was subjected to oxidation under either only 0.3 mM of initial EDTA (blank experiment without ZVI), only 90 g/L of ZVI (blank experiment without EDTA) or 90 g/L of ZVI plus 0.3 mM of initial EDTA (proof of concept), using in the three cases 10 NL/h of air flow and at 20ºC. The results are shown in Figure 2. The experiment without EDTA yielded a very low tyrosol conversion, less than 4%. This low conversion can

176 be explained by a radical mechanism. The first step of the mechanism is the corrosion of the
177 zero valent iron by the dissolved oxygen to produce hydroxyl radicals. The radicals are
178 responsible of the destruction of tyrosol like in other radical mechanisms [23-26]. As the pH
179 is well over 3 during all the experiment, the ferrous cations formed during oxidation of ZVI
180 precipitated by the formation of ferrous hydroxide. On the other hand passivation of iron
181 surface by the presence of oxide provoked that the rate of oxidation is low, showing a small
182 conversion of tyrosol (the full mechanism is described in section 3.7. Mechanism and reaction
183 intermediates).
184 The experiment without ZVI gave no significant tyrosol conversion, less than 0.6% that can
185 be attributed to experimental error. In this case, there is no production of hydroxyl radicals
186 then, no oxidation of tyrosol. As there is not chemical reaction between the two organics,
187 tyrosol and EDTA, the concentration of tyrosol is not affected.
188 Under the combination of ZVI and EDTA gave high conversion of tyrosol, 67% was achieved
189 after just 120 minutes and near 98% after 360 minutes. In this case, the mechanism is quite
190 similar than without EDTA. The first step is exactly the same. After this, by the addition of
191 EDTA to the reactive media, the ferrous cations are chelated by the EDTA and are not
192 precipitated. In a following step, the Fe^{II} iron complex is oxidised to a Fe^{III} complex allowing
193 the formation of additional hydroxyl radicals [18], increasing the reaction rate and provoking
194 a higher conversion of the tyrosol. A kind of synergy between ZVI and EDTA allowed the
195 improvement of conversion.
196 Despite the fact that ZVI and air are able to oxidise tyrosol in short quantities as elsewhere
197 demonstrated [29], where 90% of phenol conversion for an initial concentration of 25 mg/L
198 was attained, result is not satisfactory for practical purposes, so only the combination of
199 metallic ZVI, EDTA and air gives tyrosol degradation rates acceptable high enough. Based on
200 these results, the operative reaction conditions were systematically optimized.

3.2. Effect of ZVI initial load

The BET surface area of the commercial zero valent iron was around 2 $m^2 g^{-1}$. The influence of the ZVI initial mass on the tyrosol degradation was investigated at 2 mM of tyrosol, 0.3 mM of EDTA, 20ºC and 10 NL/h of air flow. Five different amounts of ZVI were added for the reactor: 10, 30, 50, 70 and 90 g/L. Figure 3a depicts the tyrosol conversion profiles obtained. The tyrosol conversion attained after 4 h of reaction was 19%, 30%, 44%, 64% and 92% with ZVI load of 10, 30, 50, 70 and 90 g/L, respectively. Using the mechanism before described in section 3.1. “Preliminary tests”, the increase of the quantity of ZVI in the reactor augments proportionally the available surface of the iron. Then, the area of contact where the dissolved molecular oxygen can oxidise the surface of the ZVI is higher, increasing the accelerating the formation of ferrous cations and of the chelate Fe^{2+}-EDTA. According to the mechanism proposed by Noradoun et al. [16], the chelated iron enhances the subsequent production of H_2O_2 and then of hydroxyl radicals. The increase of the ZVI amount improved the efficiency of the tyrosol degradation.

The amount of ZVI also influences the mineralization. Hence, TOC removal efficiency was measured after 360 minutes. The Table 2 presents the value of TOC conversions, where the TOC from EDTA was taken into account in the calculation. With low amounts of ZVI, 10 and 30 g/L, low values of conversion of tyrosol were attained, but almost nil mineralization. In the above conditions the peroxide generated preferentially attacks the tyrosol as the concentration of intermediates is too low. When the amount of ZVI increases, as there is progressive excess of peroxide and then of hydroxyl radicals, the tyrosol conversion is higher and more intermediates are produced, increasing the tyrosol conversion up to total conversion. Meanwhile, the intermediates produced by the destruction of tyrosol are available for further oxidation, producing other intermediates of lower molecular weight until they are eventually

fully mineralized to CO_2, increasing TOC conversion up to total conversion. To attain this TOC total conversion, at least the stoichiometric quantity of radicals should be produced by the process. In fact, the excess of ZVI did not provoke an inhibition of the system as observed elsewhere [17]. It was possible that an excess of ZVI would decrease the concentration of hydrogen peroxide, then hydroxyl radicals or, react with the oxidants present in the reactor. For that reason, it is required to keep in the reactor an optimal ZVI concentration during the tyrosol and EDTA degradation.

Figure 3b shows the pH evolution during the reaction. After adding the ZVI, the pH increases in the first 10 minutes from the original pH 5.2 up to pH 6.3, 7.5, 8.0, 8.0 and 7.9 for ZVI amounts of 10, 30, 50, 70 and 90 g/L, respectively. During the reaction, the pH of the solution decreased in a small range for the three higher ZVI amounts, which should mean that some intermediates of the oxidation are formed, presumably short chain organic acids, like acetic or formic acids. With the ZVI amount of 10 and 30 g/L, the pH of solution increased slowly during the reaction. This fact confirms that with low amounts of ZVI there is no production of intermediates and no mineralization of tyrosol. For all the ZVI amounts, after 120 minutes of reaction, the solution pH got to a platform in the range of 7.0 to 7.5. The formation of reaction intermediates provoked a self-buffering of the solution, helped by the presence of EDTA, preventing big changes of the pH during the reaction [16]. In conclusion of the study of the effect of initial ZVI initial load, the best amount of ZVI for an initial concentration of tyrosol of 2 mM was 90 g/L. Taking in account this result, in the continuation of the optimization study, the amount of 90 g/L of ZVI will be set.

3.3. Effect of the temperature

Tyrosol oxidation experiments at 20, 30, 40 and 50ºC were conducted to evaluate the influence of the temperature. The rest of conditions were kept: 2 mM of tyrosol, 90 g/L of

ZVI, 0.3 mM of EDTA and 10 NL/h of air flow. Figure 4 displays the conversion evolution against the reaction time. The mechanism of the process is exactly the same than in sections 3.1. “Preliminary tests” and 3.2. “Effect of ZVI initial load”. The major difference between these sections and the study of the effect of the temperature affects kinetics. As expected by the kinetics of the system, that has to be consistent with the Arrhenius law (equations 6, 7 and 9 of the section 3.8. “Kinetics”). An increase of temperature provoked an augment of the rate constant and then of the tyrosol disappearance rate followed by an increase of the conversion of tyrosol. The enhancement of conversion was high, after 60 minutes of reaction: 38% at 20ºC, 55% at 30ºC, 75% at 40ºC and 92% at 50ºC. For the two higher temperatures, quasi total tyrosol conversion was attained after only 120 minutes. Kinetic values of Arrhenius equation were calculated and are presented in section 3.9. Kinetics.

The Table 3 presents the value of TOC conversion after 360 minutes of reaction. The enhancement of TOC conversion is not as significant as for tyrosol conversion. It is expected that the remaining TOC contains intermediates of the oxidation of both tyrosol and EDTA, formed presumably by short chain organics, like acetic or formic acids from tyrosol and glyoxilic or oxalic acids from EDTA.

Although a higher temperature, from a practical point of view, means higher operating cost, the temperature range studied can still be considered as mild conditions. Taking into account the Mediterranean climate, we selected 30ºC for the subsequent tests as it could require minimum heating of the wastewater but it gives already a high degradation rate.

3.4. Effect of initial EDTA concentration

To assess the influence of the initial EDTA concentration on the tyrosol removal, the oxidation process was studied using four concentrations: 0.15, 0.30, 0.45 and 0.60 mM. In turn, two initial concentrations of tyrosol were used: 2 and 4 mM. The other reaction

conditions were maintained: 90 g/L of ZVI, 30ºC and 10 NL/h of air flow. Figures 5a and 5b show the tyrosol conversion evolution for 2 and 4 mM of EDTA, respectively. As evidenced, the initial EDTA concentration greatly affects the tyrosol conversion. However, the highest EDTA concentration, 0.60 mM, only slightly improves the performance using 0.45 mM and a short time. This result agrees with the results of Noradoun and Cheng [18] because the initial concentration of EDTA is below 1.00 mM where the degradation rate of EDTA began to decrease. With 0.60 mM of EDTA the experiment was in the conditions where the degradation of EDTA is higher then the availability to degrade tyrosol lower.

Almost complete tyrosol conversion was attained for 2 mM of tyrosol and 0.30 mM of EDTA (300 minutes), 0.45 and 0.60 of EDTA (after only 120 minutes). These results were obtained despite the EDTA is degraded too. In fact, the intermediates of degradation of EDTA, nitrilotriacetic acid (NTA) or iminodiacetic acid (IMDA), can also act as a chelating agent and are able to maintain the oxidation of tyrosol [19]. For this reason, this process has interest, the degradation of the ZEA catalytical system is maintained by the degradation products, NTA or IMDA, allowing high tyrosol degradation.

The increase of the initial concentration of tyrosol supposed a decreased in the final conversion attained after 240 minutes, but the value attained with 0.45 mM of EDTA, 94%, was notable. The augment of the initial concentration of tyrosol did not suppose a big inconvenient to attain high conversions. An additional experiment realised with 8 mM of tyrosol initial concentration attained a conversion of 63% after 240 minutes, reaffirming the potential of the ZEA system. The most remarkable values were 50% of conversion for 0.60 mM after 30 minutes and 77% after 60 minutes for 0.45 and 0.60 mM of EDTA initial concentration (tyrosol of 2 mM). If the ratio between tyrosol and EDTA is large enough, high tyrosol conversion are attained because degradation products of EDTA maintain catalytical effect.

On the other hand, TOC reduction after 360 minutes was for 2 mM of tyrosol: 48, 80, 84 and 82% with initial EDTA concentrations of 0.15, 0.30, 0.45 and 0.60 mM, respectively and, after 240 minutes was for 4 mM of tyrosol: 21, 42 and 70% with initial EDTA concentrations of 0.15, 0.30, and 0.45 mM, respectively. Again, the effect on mineralization was less remarkable than for tyrosol conversion.

To summarize, the increase of EDTA initial concentration positively influences on the tyrosol conversion noticeable up to 0.45 mM of EDTA, beyond this value only marginal improvement was found. Therefore, 0.45 mM EDTA was set for further testing.

3.5. Effect of initial pH

The influence of the pH on the tyrosol oxidation in the ZEA oxidation system was studied by varying the starting pH from 2 to 10. In this set of experiments, the experiments were stopped after 4 h as total conversion was rapidly achieved. The rest of conditions were not modified: 2 mM of tyrosol, 90 g/L of ZVI, 0.3 mM of EDTA, 30ºC and 10 NL/h of air flow. Figure 6a shows the tyrosol conversion profiles for several initial pH. It was found that tyrosol can be almost fully eliminated in the pH range between 3 and 6 after just 120 minutes. At an initial pH of 8, tyrosol conversion was still 88% after 120 minutes, and reached 100% after 180 minutes. Finally, tyrosol was totally removed after 4 h starting from an initial pH of 10, although a long induction period is observed. In fact, the ZEA process can be considered as an enhanced Fenton-like process as some of its characteristics can be observed here. The decrease of the pH promotes the conversion of tyrosol, and as in a Fenton system. But, the ZEA process is able to work in a larger range pH 2-10 when, in the traditional Fenton reaction systems, the reaction must be carried out in the narrow range 3-5 of pH, because the inability of the homogeneous iron to remain in solution beyond pH 4. As in a Fenton process, at pH 2 the conversion of tyrosol was lower than at ph 3, provoked by the inhibition of the process.

The ability of the ZEA system to work in a wide range of pH can be explained by the utilisation of a chelant. The EDTA prevents the precipitation of iron in the solution at higher pH (6.0-7.0) by forming stable chelates with iron ions, promoting its availability for hydroxyl radical generation in a wider pH range [30]. For this reason, tyrosol conversions attained at pH 8 and 10 are remarkable. This fact has a great interest as the ZEA system does not require previous acidification of the often caustic industrial effluents.

Figure 6b shows the results of TOC removal from different initial pH. In general, TOC removal follows the same trends than tyrosol conversion. Thus, pH 3, 4 and 5 gave the best TOC conversions, all more than 40% after 60 minutes, more than 70% after 120 minutes and more than 80% after 180 minutes. When the pH increased, the TOC reduction rate decreased, however, TOC removal was able to attain 80%, 78% and 68%, after 240 minutes of reaction, with initial pH of 6, 8, and 10 respectively. Again, from the above results, as commented in previous section, it can be supposed that most of the tyrosol and EDTA in the system was completely degraded into CO_2.

Finally, Figure 6c shows the pH evolution during the oxidation of tyrosol. As it can be examined in the figure, the pH end value of the treated solution after reaction is independent from the initial acidity of the solution. For the experiments with an initial pH within 3 to 8, the pH increased in the beginning of the reaction, and then decreased to reach a pH value close to 7.7. In the case of the initial pH of 2, the pH end value increased to 6 and it was stabilized at this value for the 240 minutes of the experiment. With an initial pH of 10, the pH of the solution decreased to pH 8.5 and then was stabilized. Except for the case of initial pH 2, the effect of adjust initial pH has not great effect on the pH during last 180 minutes of experiment. As it was stated, the production of intermediates of reaction provokes by their nature a self-buffering of the reaction media avoiding big changes in the pH [18].

3.6. Effect of initial concentration of tyrosol

Finally, the effect of the initial concentration of tyrosol was investigated. The initial concentrations used were 2, 4 and 8 mM (280, 560 and 1120 ppm). The other operating conditions were maintained: 90 g/L of ZVI, 0.45 mM of EDTA, 30ºC 10 NL/h of air flow. Figure 7 illustrates the results of tyrosol conversion as a function of the initial concentration of tyrosol. After 240 minutes, the conversions attained were respectively 100, 94 and 63% for 2, 4 and 8 mM. More interestingly, after 60 minutes of reaction, the conversions were 76, 54 and 27%. As it was the case in a previous work with other organics [27], the conversion of tyrosol achieved with different initial concentrations of tyrosol was not the same. This trend demonstrated that the kinetics did not follow a first order reaction with respect to tyrosol, since then the conversion should be independent of the initial concentration.

Additionally, TOC reduction after 240 minutes was: 44, 70 and 80% with initial tyrosol concentrations of 2, 4 and 8 mM, respectively. Another time, the enhancement on mineralization was less important than for tyrosol conversion. Again, this tendency proves that the kinetics are not first order respect to tyrosol. A more detailed study of this behaviour will be presented in section 3.8 kinetics.

3.7. Reaction intermediates

As seen above, total mineralization is not achievable in the ZEA system. For instance, there was 80% TOC removal at 30ºC, 0.45 mM EDTA, 90 g/L Fe after 4 h. The analysis of the samples to identify intermediates of reaction allowed to identify 3,4-dihydroxyphenylethanol, 3,4-dihydroxyphenylacetic acid and 3,4-dihydroxymandelic acid in the first stage of the oxidation. As the oxidation progresses, these first intermediate compounds were further degraded and remnant sample showed the occurrence of small molecular weight organic acids, mainly acetic, formic, pyruvic and succinic acids. Only these 7 organics were identified

as product intermediates of the oxidation of tyrosol but there must be many more.

As tyrosol is in fact 4-(2-Hydroxyethyl) phenol, the degradation products from its oxidation should follow a similar pathway than phenol. In this pathway, 21 intermediates were needed to describe the total mineralization of phenol to carbon dioxide and water [31]. In the study, only 15 of the organic intermediates were identified in the reaction products.

The identification of 3,4-dihydroxyphenylethanol, 3,4-dihydroxyphenylacetic acid and 3,4-dihydroxymandelic acid shows that the degradation mechanism of tyrosol is similar than phenol, where hydroxyl groups are added to the tyrosol molecule before opening the ring or breaking the 2-hydroxyethyl chain. Acetic, formic and succinic acids, identified in the oxidation of tyrosol, were also identified in the phenol degradation pathway. Acetic and formic acids are very stable and therefore were easily identified. On the other hand, their stability also signifies that they are complicated to further degrade. The presence of succinic acid can be considered as a side reaction because its production needs the hydrogenation of the carbon to carbon double bonds of the maleic acid, not detected here [31]. The pyruvic acid is a specific degradation product of the tyrosol pathway, but its structure is similar than glyoxilic acid, but with a methyl group. It should be produced by oxygen attack of double bonds from a structure like maleic or acrylic acids, with a methyl group chained to their structure. On the other hand, the degradation of EDTA should produce intermediates of the reaction as nitrilotriacetic acid or iminodiacetic acid [17], not identified in this work.

3.8. Mechanism

The high values of TOC conversion attained in some experiments, TOC from tyrosol and EDTA, indicates that tyrosol and EDTA are nearly entirely destroyed in ZEA system and a considerable amount of them were mineralized and only a fraction was converted to lower mass organic products, which can be easily destroyed by biodegradation methods [32]. The

401 mechanism of degradation of both tyrosol and EDTA is expected to follow similar pathways
402 previously described [17]. This mechanism is illustrated in Figure 8, where competition for
403 organics is observed. In the case of real OMW, that consists of hundreds of different organics
404 with high molecular weight, the mechanisms for each organic should be similar. However, the
405 rates should not be exactly the same than for tyrosol, giving to the treatment a greater
406 complexity.
407 On the other hand, Figure 9 shows the concentration of iron cations in dissolution during
408 degradation of tyrosol. In principle, the presence of iron ions in solution shows that the
409 mechanism actually works. The amount of ferrous ions increased very quickly during the first
410 60 minutes but, after peaking, the value decreased rapidly. At short times, the higher the load
411 of EDTA, the higher the concentration of iron cations but, after 120 minutes, the values were
412 equal for the four experiments. According to Zhou et al. [17], the first step in the mechanism
413 is the iron corrosion in aqueous media:

414 $$Fe^0 + H_2O + \tfrac{1}{2}O_2 \rightarrow Fe^{2+} + 2OH\cdot \quad (1)$$

415 Then, ferrous cations are chelated by EDTA:

416 $$Fe^{2+} + EDTA \leftrightarrows [Fe^{II}(EDTA)]^{2+} \quad (2)$$

417 The oxidation of Fe^{II}-EDTA complex in solution allows the formation of additional hydroxyl
418 radicals [17]:

419 $$[Fe^{II}(EDTA)]^{2+} + \tfrac{1}{2}O_2 + H_2O \rightarrow [Fe^{III}(EDTA)]^{3+} + OH\cdot \quad (3)$$

420 The hydroxyl radicals formed oxidize both the contaminant (Tyrosol) and EDTA itself.
421 Usually, the process should continue working as long as there had available iron but, this was
422 not the case. The surface of the metallic iron particles probably become covered by iron
423 oxide, products or intermediates, provoking the surface passivation. Additionally, Fe^{III} ions
424 could precipitate as $Fe(OH)_3$ as the pH is over 2-3, mainly if not enough EDTA is available.
425 On the other hand, the saturation of the complex in solution should be attained as equilibrium

426 eq. 3 describes. All these facts explain that the oxidation performance decline at long time.

427

428 **3.9. Kinetics.**

429 A kinetic analysis of the process was performed. Individually, the experiments varying
430 temperature, initial EDTA, ZVI or Tyrosol concentration, fitted a pseudo first order behaviour
431 (data not shown). However, the tyrosol conversion obtained starting from different initial
432 tyrosol concentrations were not the same, as expected for a pure first order reaction, where the
433 conversion is independent of the initial concentration. Therefore, a deeper evaluation was
434 required. For the catalytic oxidation of aqueous organic pollutants, the kinetic models
435 proposed in the literature are in terms of either power laws or more complex equations based
436 on adsorption-desorption mechanisms, i.e., Langmuir-Hinshelwood (LH) model [33],
437 expressed by eq (4):

438
$$-r = \frac{k_0 \cdot [Ty]}{1 + K_1 \cdot [Ty]} \tag{4}$$

439 Where r is the global reaction rate, [Ty] the tyrosol concentration, k_0 the rate constant and K_1,
440 the adsorption equilibrium constant.
441 As it was guessed, EDTA plays an important role in the reaction because it combines with
442 ferrous cations to form a metallic chelate that activates the oxygen to produce hydrogen
443 peroxide and hydroxyl radicals [17]. As a higher initial rate of tyrosol destruction resulted
444 from a higher oxidative system concentration, the EDTA initial concentration and the ZVI
445 mass should be considered in the kinetics expression.
446 Therefore, the tyrosol disappearance rate was now written including terms of EDTA
447 concentration (not considered constant as also it is degraded), initial ZVI concentration and
448 dissolved oxygen concentration, considered constant for all experiments, eq (5).

449
$$-r = \frac{k_0 \cdot [Ty] \cdot [EDTA] \cdot f(m_{ZVI}) \cdot [O_2]_{dis.}}{1 + K_1 \cdot [Ty]} \tag{5}$$

Where k_0 is the rate constant, [EDTA] the concentration of EDTA, $[O_2]_{dis.}$ the dissolved oxygen concentration and $f(m_{ZVI})$ an exponential function of initial mass of ZVI. This relationship was established after the determination of tyrosol degradation rate constants, varying the ZVI concentration. The function was confirmed with the values obtained elsewhere [17].

On the other hand, k_0 and K_1 have to be consistent with the Arrhenius law, eq (6) and (7).

$$\ln k_0 = \ln A_0 - \left(\frac{E_0}{R.T}\right) \quad (6)$$

Where A_0 is the pre-exponential factor of the rate constant and E_0 is the activation energy.

$$\ln K_1 = \ln A_1 - \left(\frac{E_1}{R.T}\right) \quad (7)$$

Where A_1 is the pre-exponential factor of the adsorption equilibrium constant and E_1 is the activation energy.

As the process also degrades EDTA, eq (8).

$$-r_{EDTA} = k_{EDTA} \cdot [EDTA] \cdot f(m_{ZVI}) \cdot [O_2]_{dis.} \quad (8)$$

Where k_{EDTA} is the rate constant for the EDTA disappearance, which also must be consistent with the Arrhenius law, eq (9).

$$\ln k_{EDTA} = \ln A_{EDTA} - \left(\frac{E_{EDTA}}{R.T}\right) \quad (9)$$

Where A_{EDTA} is the pre-exponential factor of the EDTA degradation rate constant and E_{EDTA} is the activation energy.

Equations 5 and 8 where solved together using the tool Solver of Excel®. The experiments varying temperature, initial EDTA, ZVI or Tyrosol concentration, were fitted together. Figures 10 present the fitting for the experiments varying: (a) ZVI initial mass, (b) initial temperature, (c) and (d) initial EDTA concentration and (e) initial Tyrosol concentration.

Table 4 presents the estimated values of the constants. The simulated curves are very close to the experimental values except for experiments with 0.15 mM of EDTA in Figures 10c and 10d or finally, with 2 mM of tyrosol in Figure 10e.

The activation energy obtained for k_0 was 37.7 kJ/mol. This value is close to the lower extreme of the range reported in the literature for phenol catalytic oxidation, between 37 and 118 kJ/mol [34]. The pre-exponential factor found $7.05 \cdot 10^{11}$ $L^2/mol^2 \cdot min$. The value of the k_{EDTA} obtained at 20ºC, 0.05 min^{-1}, was in the range of that presented elsewhere, 0.02 min^{-1} [18].

4. Conclusions

In the present study, degradation of tyrosol in EDTA-Fe-Air heterogeneous system was investigated. Fe-EDTA is an efficient, cheap and green Fenton like oxidation method for pollutant degradation. Tyrosol gets more than 99% conversion after 2 h reaction with 0.45 mM EDTA, 90 g/L Fe at 30ºC, and after reaction, EDTA can be degraded together with tyrosol. TOC removal is 80% after 3 h reaction with above reaction conditions. Another advantage of the ZEA system is that the degradation products of EDTA, NTA or IMDA, can also act as a chelating agent and are able to maintain the oxidation of tyrosol.

The concentration of EDTA, the concentration of Fe and temperature has a great effect on tyrosol degradation. The optimized condition is Fe 90 g/L, EDTA 0.45 mM, temperature 30ºC, reaction time 3 h. Comparing with Fenton oxidation system, Fe-EDTA oxidation system can be used in a broad pH range from 3 to 8 and the best pH range is from 3 to 6.

A simplified mechanism of degradation was presented where several intermediates were identified.

The kinetics of the process was investigated. A Langmuir-Hinshelwood model was used to fit experimental results. Activation energy was close to other phenolic compounds ones.

Tyrosol, one of the typical phenolic compounds of OMW, was efficiently degraded in ZEA system at mild conditions. The ZEA system can be considered as a promising process for the degradation of olive mill wastewater.

Acknowledgements

Financial support for this research was provided by project "CTM2008-03338" of the Spanish Ministry of Education and Science. Dongmei Fu is indebted to the Programa Beatriu de Pinos de l'Agència de Gestió d'Ajusts Universitaris i de Recerca (AGAUR) of Generalitat de Catalunya for providing a post-doctoral grant. The author's research group is recognized by the Comissionat per a Universitats i Recerca del DIUE de la Generalitat de Catalunya (2009SGR865) and supported by the Universitat Rovira i Virgili (2010PFR-URV-B2-41).

References

[1] G. Hodaifa, J.M. Ochando-Pulido, S. Rodriguez-Vives, A. Martinez-Ferez, Optimization of continuous reactor at pilot scale for olive-oil mill wastewater treatment by Fenton-like process, Chem. Eng. J. 220 (2013) 117-124.

[2] N. Azbar, A. Bayram, A. Filibeli, A. Muezzinoglu, F. Sengul, A. Ozer, A review of waste management options in olive oil production, Crit. Rev. Env. Sci. Tec. 34 (2004) 209-247.

[3] P. Paraskeva, E. Diamadopoulos, Technologies for olive mill wastewater (OMW) treatment: a review, J. Chem. Technol. Biotechnol., 81 (2006) 1475–1485.

[4] F.A. El-Gohary, M.I. Badawy, M.A. El-Khateeb, A.S. El-Kalliny, Integrated treatment of olive mill wastewater (OMW) by the combination of Fenton's reaction and anaerobic treatment, J. Hazard. Mater., 162 (2009) 1536-1541.

521 [5] E. Eroglu, I. Eroglu, U. Gunduz, M. Yucel, Effect of clay pre-treatment on
522 photofermentative hydrogen production from olive mill wastewater, Bioresour.
523 Technol. 99 (2008) 6799-6808.
524 [6] A. Agalias, P. Magiatis, A.L. Skaltsounis, E. Mikros, A. Tsarbopoulos, E. Gikas, I.
525 Spanos, T. Manios, A new process for the management of olive oil mill waste water and
526 recovery of natural antioxidants, J. Agr. Food Chem. 55 (2007) 2671-2676.
527 [7] H. Inan, A. Dimoglo, H. Simsek, A. Karpuzcu, Olive oil mill wastewater treatment by
528 means of electro-coagulation, Sep. Purif. Technol. 36 (2004) 23-31.
529 [8] R. Sarika, N. Kalogerakis, D. Mantzavinos, Treatment of olive mill effluents Part II.
530 Complete removal of solids by direct flocculation with poly-electrolytes, Environ. Int.
531 31 (2005) 297-304.
532 [9] C.A. Paraskeva, V.G. Papadakis, E. Tsarouchi, D.G. Kanellopoulou, P.G. Koutsoukos,
533 Membrane processing for olive mill wastewater fractionation, Desalination. 213 (2007)
534 218-229.
535 [10] C. Justino, A.G. Marques, K. Reis Duarte, A. Costa Duarte, R. Pereira, T. Rocha-Santos,
536 A.C. Freitas, Degradation of phenols in olive oil mill wastewater by biological,
537 enzymatic, and photo-Fenton oxidation, Environ. Sci. Pollut. Res. 17 (2010) 650-656.
538 [11] S. Khoufi, F. Aloui, S. Sayadi, Detoxification of olive mill wastewater by
539 electrocoagulation and sedimentation processes, J. Hazard. Mater. 142 (2007) 58-67.
540 [12] S. Azabou, W. Najjar, M. Bouaziz, A. Ghorbel, S. Sayadi, A compact process for the
541 treatment of olive mill wastewater by combining wet hydrogen peroxide catalytic
542 oxidation and biological techniques, J. Hazard. Mater. 183 (2010) 62-69.
543 [13] P. Aytar, S. Gedikli, M. Sam, B. Farizoglu, A. Çabuk, Sequential treatment of olive oil
544 mill wastewater with adsorption and biological and photo-Fenton oxidation, Environ.
545 Sci. Pollut. Res. 20 (2013) 3060-3067.

546 [14] A.S. Fajardo, R.C. Martins, R.M. Quinta-Ferreira, Treatment of a simulated phenolic
547 effluent by heterogeneous catalytic ozonation using Pt/Al_2O_3, Environ. Technol. 34
548 (2013) 301-311.
549 [15] R. Oztekin, D.T. Sponza, Treatment of wastewaters from the olive mill industry by
550 sonication, J. Chem. Technol. Biotechnol. 88 (2013) 212-225.
551 [16] C.E. Noradoun, M.D. Engelmann, M. McLaughlin, R. Hutcheson, K. Breen, A.
552 Paszcznski, I.F. Cheng, Destruction of chlorinated phenols by dioxygen activation
553 under aqueous room temperature and pressure conditions, Ind. Eng. Chem. Res. 42
554 (2003) 5024-5030.
555 [17] T. Zhou, T.T. Lim, Y. Li, X. Lu, F.S. Wong, The role and fate of EDTA in ultrasound-
556 enhanced zero-valent iron/air system, Chemosphere 78 (2010) 576-582.
557 [18] C.E. Noradoun, I.F. Cheng, EDTA degradation induced by oxygen activation in a
558 zerovalent iron/air/water system, Envrion. Sci. Technol. 39 (2005) 7158-7163.
559 [19] I. Sanchez, F. Stuber, A. Fabregat, J. Font, A. Fortuny, C. Bengoa, Degradation of model
560 olive mill contaminants of OMW catalysed by zero-valent iron enhanced with a chelant,
561 J. Hazard. Mater. 199-200 (2012) 328-335.
562 [20] D. Mantzavinos, N. Kalogerakis, Treatment of olive mill effluents Part I. Organic matter
563 degradation by chemical and biological processes-an overview, Environ. Int. 31 (2005)
564 289-295.
565 [21] K.L. Tuck, P.J. Hayball, Major phenolic compounds in olive oil: metabolism and health
566 effects, J. Nutr. Biochem. 13 (2002) 636-644.
567 [22] P.P. Liebgott, M. Labat, A. Amouric, J.L. Tholozan, J. Lorquin, Tyrosol degradation via
568 the homogentisic acid pathway in a newly isolated *Halomonas* strain from olive
569 processing effluents, J. Appl. Microbiol. 105 (2008) 2084-2095.

570 [23] S. Khoufi, F. Aloui, S. Sayadi, Treatment of olive oil millwastewater by combined
571 process electro-Fenton reaction and anaerobic digestionm, Water Res. 40 (2006) 2007-
572 2016.
573 [24] F. Cermola, N. DellaGreca, M.R. Iesce, S. Montella, A. Pollio, F. Temussi, A mild
574 photochemical approach to the degradation of phenols from olive oil mill wastewater,
575 Chemosphere 55 (2004) 1035-1041.
576 [25] W. Najjar, S. Azabou, S. Sayadi, A. Ghorbel, Catalytic wet peroxide photo-oxidation of
577 phenolic olive oil mill wastewater contaminants - Part 1. Reactivity of tyrosol over (Al-
578 Fe)PILC, Appl. Catal. B: Environ. 74 (2007) 11-18.
579 [26] R. Ben-Achma, A. Ghorbel, A. Dafinov, F. Medina, Copper-supported pillared clay
580 catalysts for the wet hydrogen peroxide catalytic oxidation of model pollutant tyrosol,
581 Appl. Catal. A: Gen. 349 (2008) 20-28.
582 [27] I. Sanchez, F. Stuber, J. Font, A. Fortuny, A. Fabregat, C. Bengoa, Elimination of phenol
583 and aromatic compounds by zero valent iron and EDTA at low temperature and
584 atmospheric pressure, Chemosphere 68 (2007) 338-344.
585 [28] M.E. Suarez-Ojeda, F. Stuber, A. Fortuny, A. Fabregat, J. Carrera, J. Font, Catalytic wet
586 air oxidation of substituted phenols using activated carbon as catalyst, Appl. Catal. B:
587 Environ. 58 (2005) 105-114.
588 [29] A. Shimizu, M. Tokumura, K. Nakajima, Y. Kawase, Phenol removal using zero-valent
589 iron powder in the presence of dissolved oxygen: Roles of decomposition by the Fenton
590 reaction and adsorption/precipitation, J. Hazard. Mater. 201-202 (2012) 60-67.
591 [30] G. Tachiev, J.A. Roth, A.R. Bowers, Kinetics of hydrogen peroxide decomposition with
592 complexed and “free” iron catalysts, Int. J. Chem. Kinet. 32 (2000) 24-35.
593 [31] H.R. Devlin and I.J. Harris, Mechanism of the oxidation of aqueous phenol with
594 dissolved oxygen, Ind. Eng. Chem. Fundam. 23 (1984) 387-392.

595 [32] M.E. Suarez-Ojeda, J. Carrera, I.S. Metcalfe, J. Font, Wet air oxidation (WAO) as a
596 precursor to biological treatment of substituted phenols: Refractory nature of the WAO
597 intermediates, Chem. Eng. J. 144 (2008) 205-212.
598 [33] A. Eftaxias, J. Font, A. Fortuny, J. Giralt, A. Fabregat, F. Stuber, Kinetic modelling of
599 catalytic wet air oxidation of phenol by simulated annealing, Appl. Catal. B 33 (2001)
600 175-190.
601 [34] F. Stuber, J. Font, A. Fortuny, C. Bengoa, A. Eftaxias, A. Fabregat, Carbon materials and
602 catalytic wet air oxidation of organic pollutants in wastewater, Top. Catal. 33 (2005) 3-
603 50.
604
605

606 **Notation table**

Symbol	Definition	Unit
r	Global reaction rate	mol/L·min
k_0	Tyrosol disappearance rate constant	L^2/mol^2·min
A_0	Tyrosol disappearance pre-exponential factor	L^2/mol^2·min
E_0	Tyrosol disappearance activation energy	J/mol
K_1	Adsorption equilibrium constant	L/mol
A_1	Adsorption equilibrium pre-exponential factor	L/mol
E_1	Adsorption equilibrium activation energy	J/mol
r_{EDTA}	EDTA disappearance reaction rate	mol/L·min
k_{EDTA}	EDTA disappearance rate constant	L/mol·min
A_{EDTA}	EDTA disappearance pre-exponential factor	L/mol·min
E_{EDTA}	EDTA disappearance activation energy	J/mol
[Ty]	Tyrosol concentration	mol/L
[EDTA]	EDTA concentration	mol/L
$f(m_{ZVI})$	Exponential function of initial mass of ZVI	none
$[O_2]_{dis}$	Dissolved oxygen concentration	mol/L
R	Gas constant	J/mol·K
T	Temperature	K

607

608

609

Figure captions

Figure 1. Schematic diagram of the reactor.

Figure 2. Evolution of the tyrosol degradation with time at different concentrations of ZVI and EDTA. $[Tyrosol]_0$: 2 mM, air: 10 NL/h, free pH and temperature: 20ºC.

Figure 3. Effect of ZVI initial concentration, (a) on the conversion of tyrosol and (b) on the evolution of pH. $[Tyrosol]_0$: 2 mM, $[EDTA]_0$: 0.30 mM, air: 10 NL/h, free pH and temperature: 20ºC.

Figure 4. Effect of initial temperature on the conversion of tyrosol. $[Tyrosol]_0$: 2 mM, $[ZVI]_0$: 90 g/L, $[EDTA]_0$: 0.30 mM, air: 10 NL/h and free pH.

Figure 5. Effect of initial EDTA concentration on the conversion of tyrosol, (a) $[Tyrosol]_0$: 2 mM and (b) $[Tyrosol]_0$: 4 mM., $[ZVI]_0$: 90 g/L, air: 10 NL/h, free pH and temperature: 30ºC.

Figure 6. Effect of initial pH, (a) on the conversion of tyrosol, (b) on the conversion of TOC and (c) on the evolution of pH. $[Tyrosol]_0$: 2 mM, $[ZVI]_0$: 90 g/L, $[EDTA]_0$: 0.45 mM, air: 10 NL/h and temperature: 30ºC.

Figure 7. Effect of initial tyrosol concentration on the conversion of tyrosol. $[ZVI]_0$: 90 g/L, $[EDTA]_0$: 0.45 mM, air: 10 NL/h, free pH and temperature: 30ºC.

Figure 8. Scheme of the mechanism of the degradation process adapted from Zhou et al., 2010.

Figure 9. Evolution of Fe^{II} specie during experiments. . $[Tyrosol]_0$: 4 mM and 8 mM, $[ZVI]_0$: 90 g/L, $[EDTA]_0$: 0.15, 0.30 and 0.45 mM, air: 10 NL/h, free pH and temperature: 30ºC.

Figure 10. Fitting of experimental results of tyrosol conversion depending of (a) of ZVI initial concentration, (b) initial temperature; (c) initial EDTA concentration ($[Tyrosol]_0$: 2 mM), (d) initial EDTA concentration ($[Tyrosol]_0$: 4 mM) and (e) initial tyrosol concentration.

635

636 Table 1. Chemical properties of Tyrosol and EDTA.

Compound	**Tyrosol**	**EDTA**
Molecular formula	$C_8H_{10}O_2$	$C_{10}H_{16}N_2O_8$
Molar mass (g/mol)	138.16	292.24
Chemical structure	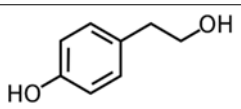	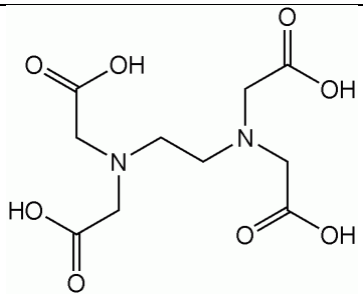

637

638

639 Table 2. Effect of ZVI initial concentration on the conversion of TOC. $[Tyrosol]_0$: 2 mM, $[EDTA]_0$: 0.30 mM,

640 air: 10 NL/h, free pH and temperature: 20ºC.

	$[ZVI]_0$ (g/L)				
	10	**30**	**50**	**70**	**90**
X_{TOC} (%)	0	0	23	43	74

641

642

643 Table 3. Effect of temperature on the conversion of TOC. $[Tyrosol]_0$: 2 mM, $[ZVI]_0$: 90 g/L, $[EDTA]_0$: 0.30

644 mM, air: 10 NL/h and free pH.

	Temperature			
	20	**30**	**40**	**50**
X_{TOC} (%)	74	80	82	83

645

646

647 Table 4. Values of the kinetic constants obtained by numerical calculation.

Equation	Constant	Value	Units
$\ln k_0 = \ln A_0 - \left(\frac{E_0}{R.T}\right)$	A_0	$7.05 \cdot 10^{+11}$	$L^2/mol^2 \cdot min$
	E_0	37700	J/mol
$\ln K_1 = \ln A_1 - \left(\frac{E_1}{R.T}\right)$	A_1	$7.70 \cdot 10^{-1}$	L/mol
	E_1	-18660	J/mol
$\ln k_{EDTA} = \ln A_{EDTA} - \left(\frac{E_{EDTA}}{R.T}\right)$	A_{EDTA}	$5.00 \cdot 10^{+6}$	L/mol·min
	E_{EDTA}	45000	J/mol

648

649

650

651 Figure 1

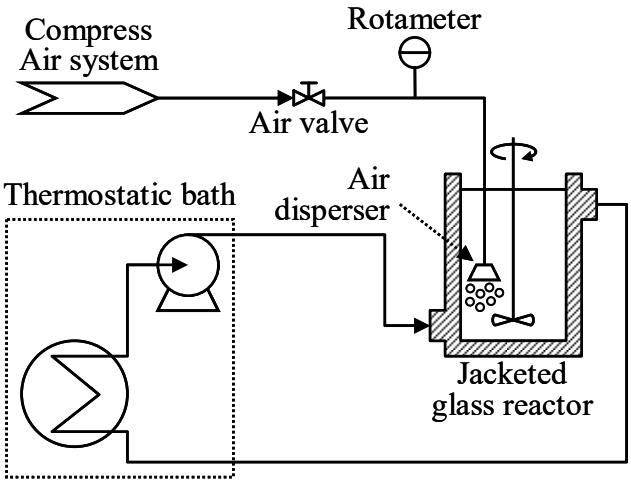

652

653

654 Figure 2

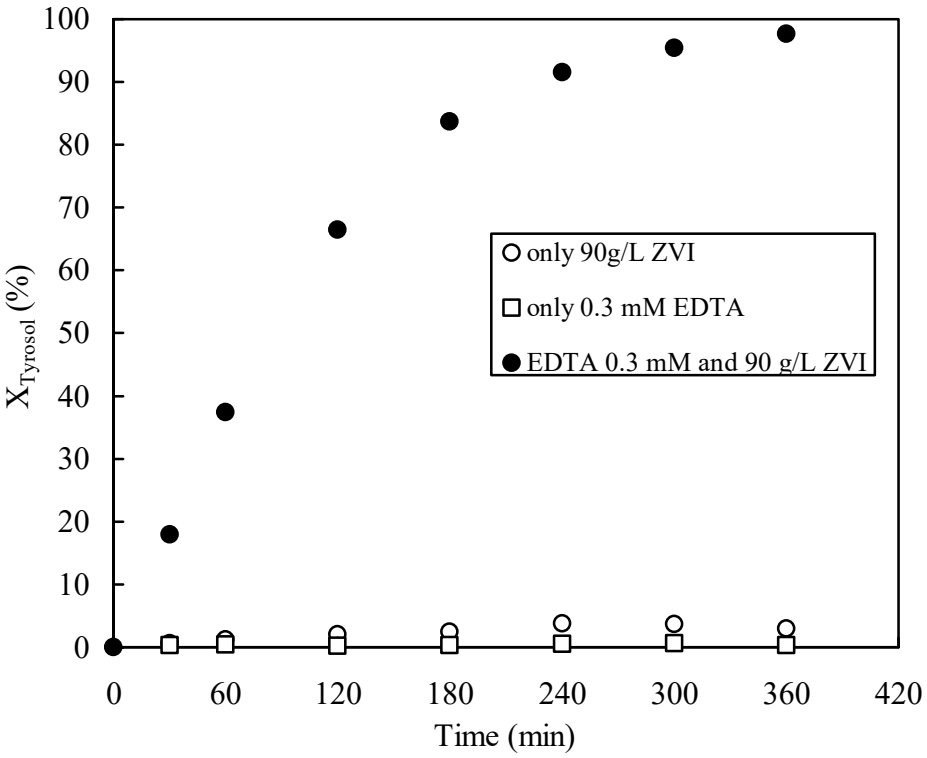

655

656

657 Figure 3

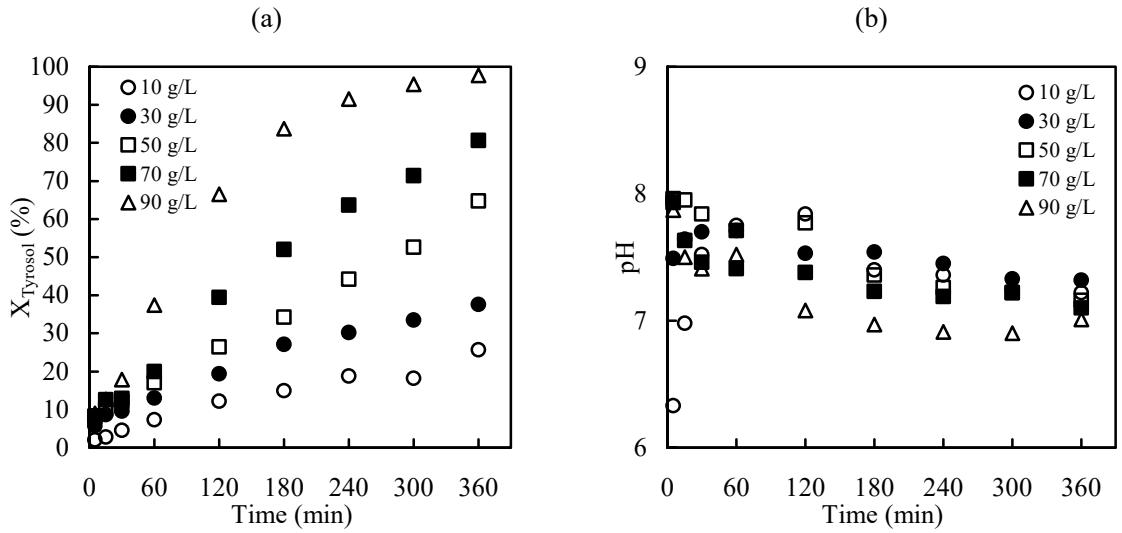

658

659

660 Figure 4

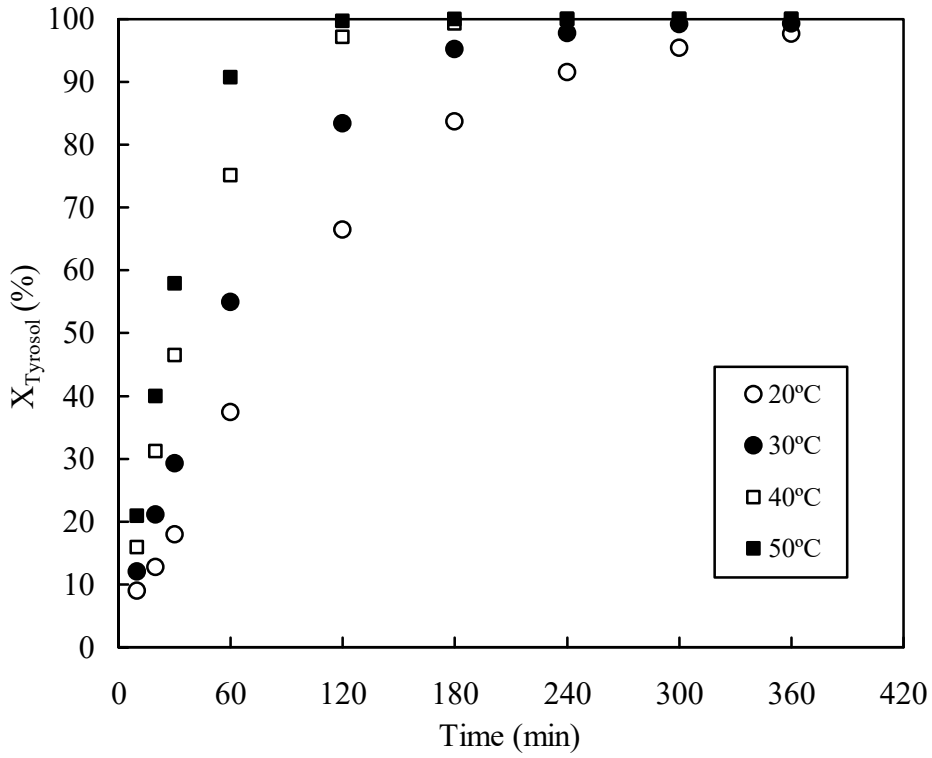

661

662

663 Figure 5

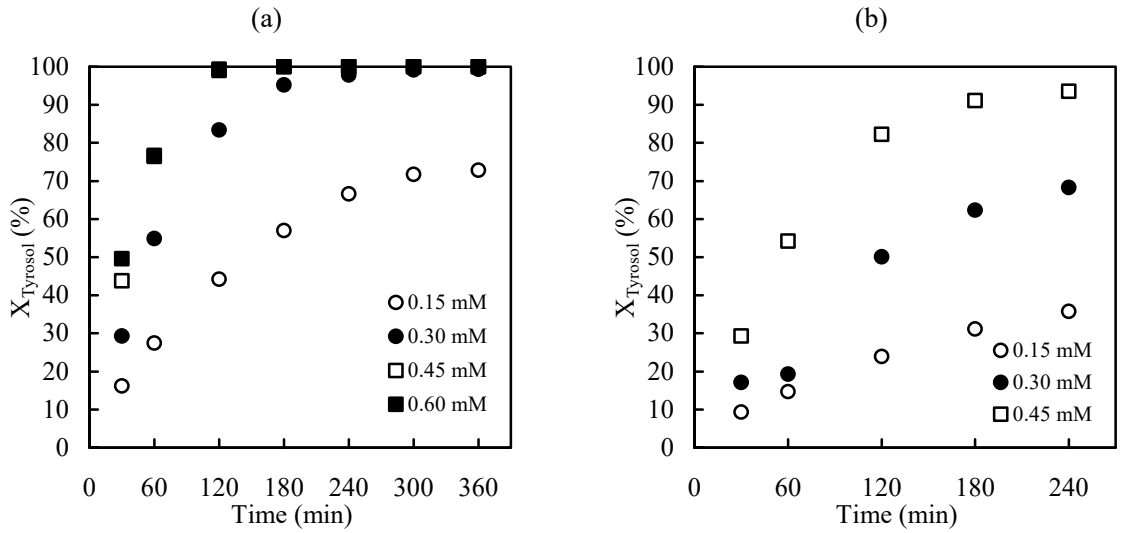

664

665

666 Figure 6

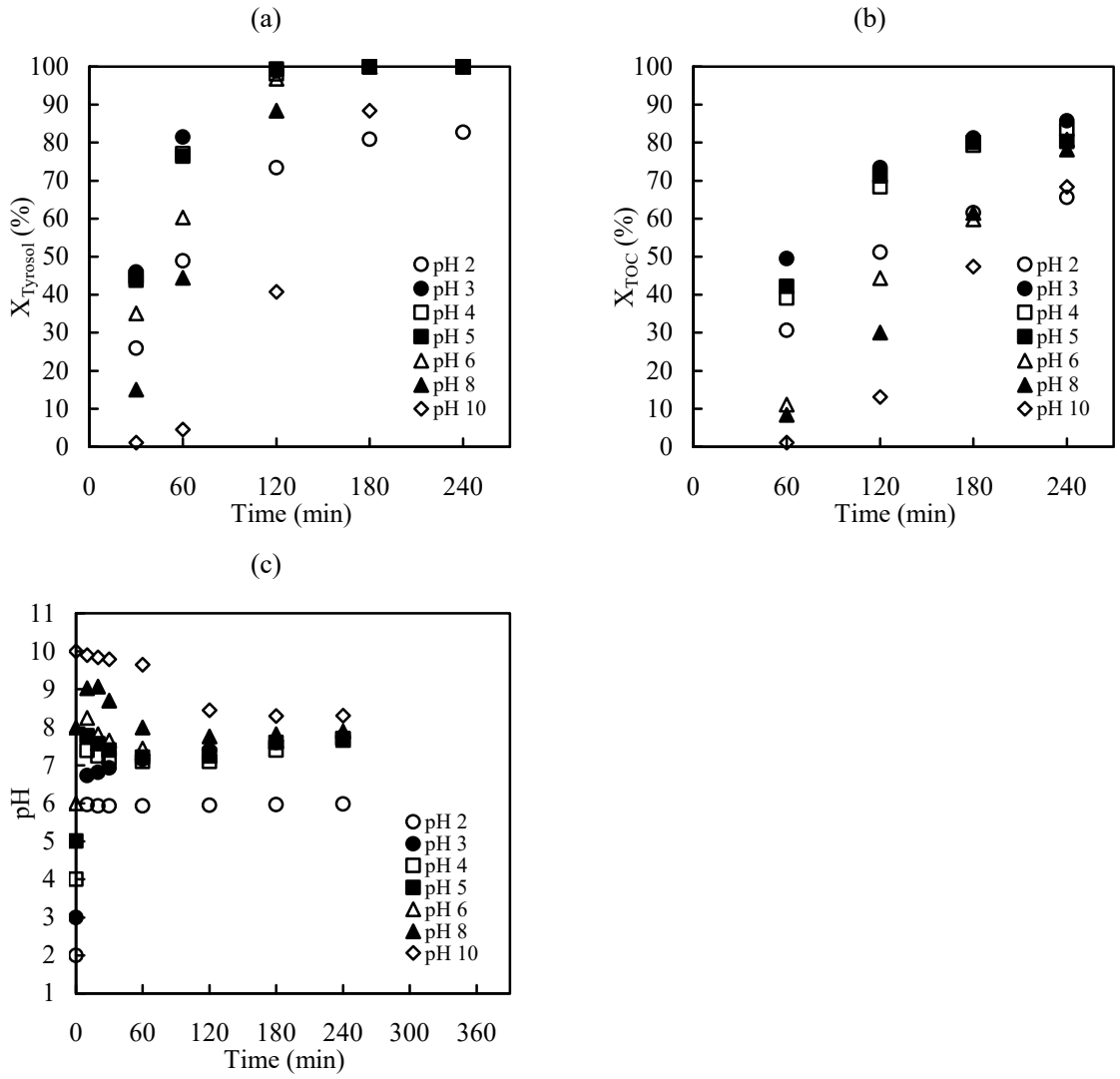

667

668

669 Figure 7

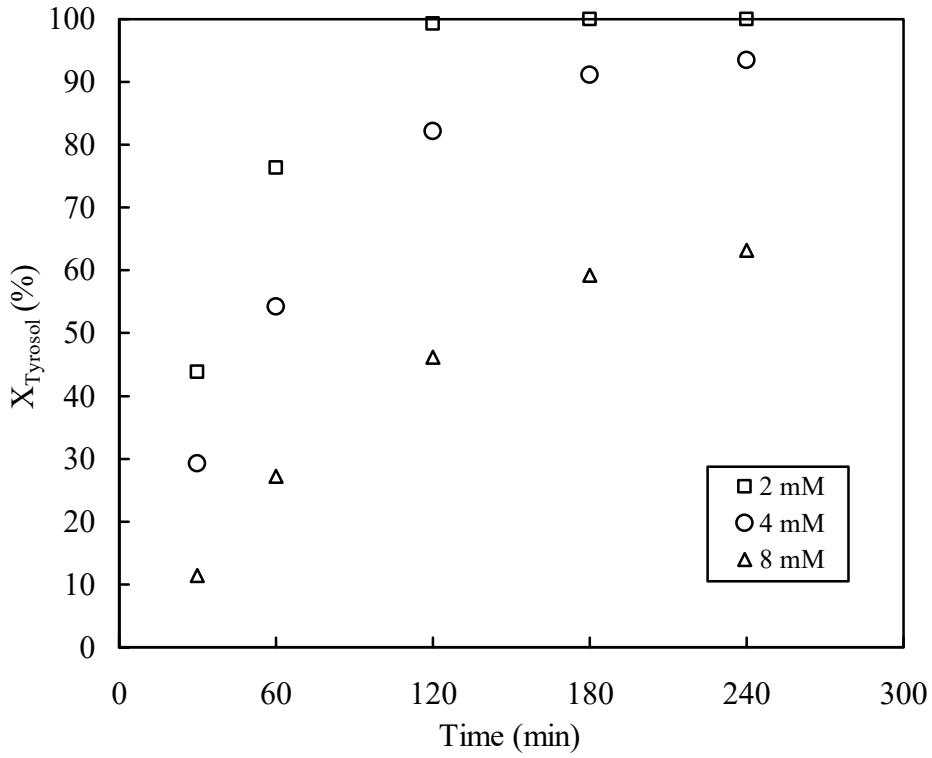

670

671

672 Figure 8

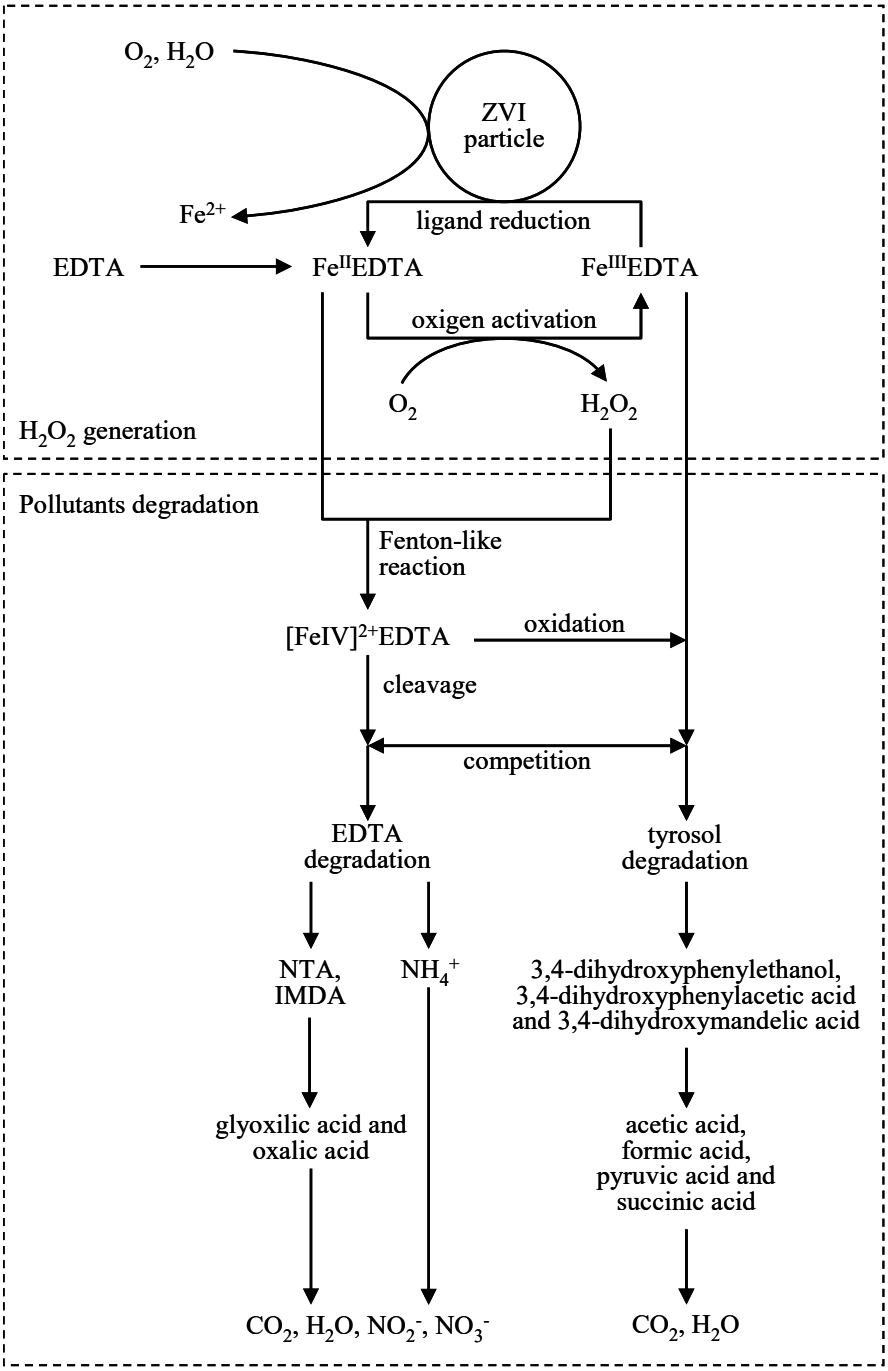

673

674

675 Figure 9

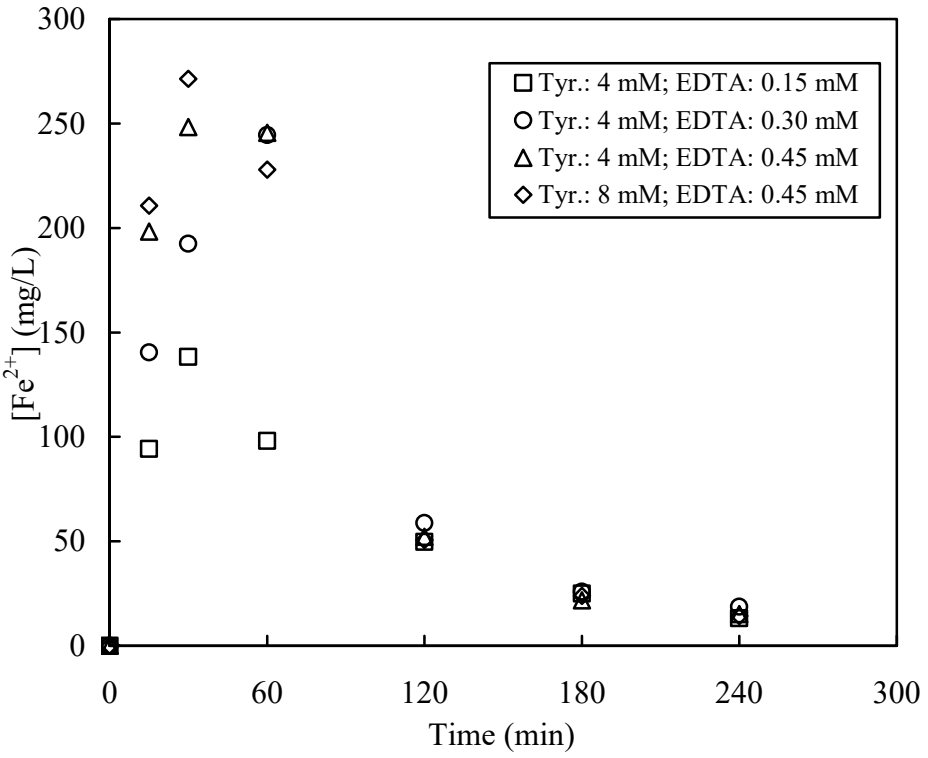

676

677

678 Figure 10

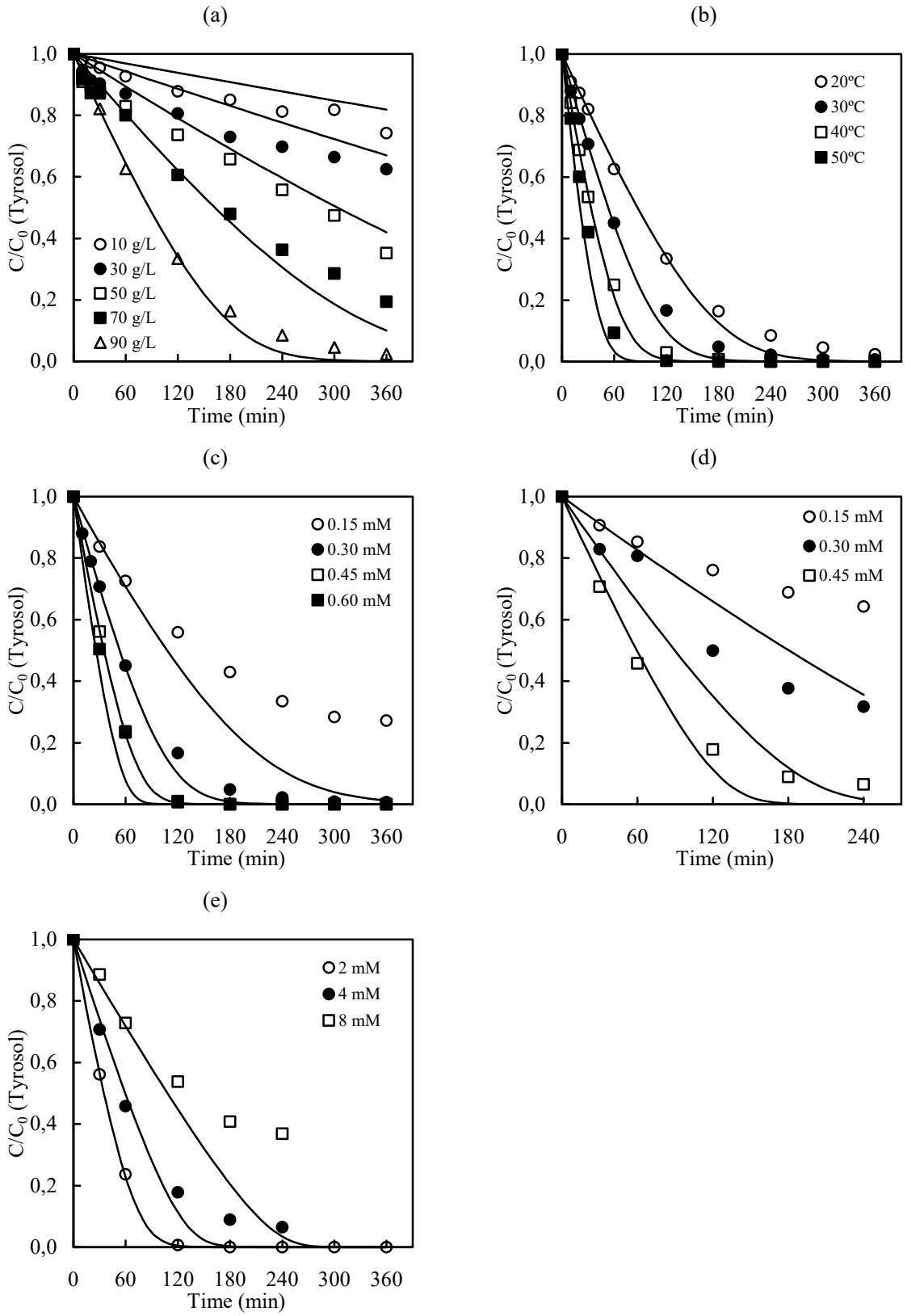

679